Cerebral Cortex July 2007;17:1542–1549
doi:10.1093/cercor/bhl063
Advance Access publication August 28, 2006

Opposite Dependencies on Visual Motion Coherence in Human Area MT+ and Early Visual Cortex

Barbara Händel[1,2], Werner Lutzenberger[3], Peter Thier[2] and Thomas Haarmeier[1,2]

Departments of [1]General Neurology and [2]Cognitive Neurology, Hertie-Institute for Clinical Brain Research and [3]Institute of Medical Psychology and Behavioural Neurobiology, University of Tübingen, 72076 Tübingen, Germany

In order to understand the relationship between brain activity and visual motion perception, knowledge of the cortical areas participating in signal processing alone is insufficient. Rather knowledge on how responses vary with the characteristics of visual motion is necessary. In this study, we measured whole brain activity using magnetoencephalography in humans discriminating the global motion direction of a random dot kinematogram whose strength was systematically varied by the percentage of coherently moving dot elements. Spectral analysis revealed 2 components correlating with motion coherence. A first component in the low-frequency domain (~3 Hz), linearly increasing with motion coherence, could be attributed to visual cortex including human area middle temporal (MT) +. A second component oscillating in the alpha frequency range and emerging after stimulus offset showed the inverse dependence on motion coherence and arose from early visual cortex. Based on these results, we first of all conclude that motion coherence is reflected in the population response of human extrastriate cortex. Second, we suggest that the occipital alpha activity represents a gating mechanism protecting visual motion integration in later cortical areas from disturbing upcoming signals.

Keywords: alpha oscillations, area MT, early visual cortex, magnetoencephalography, visual motion perception

Introduction

Sensory information is often unreliable, ambiguous, or contaminated by disturbing signals, thus, necessitating a trade-off between alternative interpretations in order to come up with a consistent perceptual decision that may guide behavior. One central goal of neuroscience is to uncover the neuronal mechanisms underlying this transformation of noisy sensory information into a uniform percept. In this field of research, combined electrophysiology and psychophysics in nonhuman primates have provided an excellent opportunity to study how properties of single neurons or of assemblies of neurons contribute to perception. The most intriguing insights in this respect have been gained from studies investigating the mechanisms underlying visual motion perception. For this, 2-alternative forced choice paradigms requiring the monkey to extract a global motion signal embedded in noise have been used in order to search for neural activity reflecting the physical properties of the stimulus, the animal's perceptual choice, or both. Specifically, by varying the difficulty of the task, that is, the percentage of elements of the random dot stimulus moving coherently in one direction (motion coherence), it has become possible to compare psychometric and neurometric functions in a quantitative manner (e.g., Newsome and others 1989). Following this approach, numerous studies have been performed to provide a detailed description of the dependencies of single-cell responses on visual motion coherence with positive (linear) correlations observed in area middle temporal (MT)/V5 (Newsome and others 1989; Britten and others 1992, 1996), area lateral intraparietal (LIP) (Shadlen and others 1996; Shadlen and Newsome 2001; Roitman and Shadlen 2002; Gold and Shadlen 2003), prefrontal areas including the frontal eye field (Kim and Shadlen 1999; Gold and Shadlen 2000), and the superior colliculus (Horwitz and Newsome 1999). Moreover, responses of neurons in area MT to random dot stimuli have been shown to carry directional signals of sufficient precision to account for the psychophysical sensitivity to visual motion (Britten and others 1992).

Whereas studies of nonhuman primates have contributed substantially to our current knowledge of the neurophysiological responses underlying motion perception, human studies measuring brain activity based on the responses of large neuronal populations are far from providing the same quantitative description of brain activity reflecting the physical properties of visual motion. Indeed, imaging studies testing human brain activity as a function of visual motion strength are sparse and, moreover, have yielded contradictory results so far. To our knowledge, 4 studies up to now measured brain activations for motion stimuli whose strength was varied systematically and demonstrated a positive correlation between responses of area MT+ and motion coherence (functional magnetic resonance imaging [fMRI], Rees and others 2000; magnetoencephalography [MEG], Nakamura and others 2003; Aspell and others 2005; Siegel and others 2006). Whereas few more studies observed a higher activity in area MT+ for coherent motion as compared with motion noise (fMRI, Braddick and others 2001; MEG, Maruyama and others 2002), other studies failed to reveal this difference or even observed the opposite dependency (McKeefry and others 1997; Lam and others 2000). The goal of the present study was to further the characterization of the population responses of motion sensitive areas by measuring how neuromagnetic cortical activity varies with the characteristics of visual motion. Particular emphasis was placed on the spectral analysis of the responses, thus, providing a full description of the dependencies of spectral powers recorded with whole-head MEG in man on motion coherence. As will be shown, we observed activations in 2 frequency domains depending on motion coherence, a first one in the low-frequency domain increasing with motion coherence and arising from extrastriate cortex and a second one in the alpha frequency range which could be attributed to early visual cortex and which showed the opposite dependency. From this pattern of results, we conclude that the integration of visual motion information over time is protected from disturbing signals via a gating mechanism implemented in early visual cortex.

Materials and Methods

Sixteen healthy subjects, 6 males and 10 females, with a mean age of 26 ± 2.9 ranging from 22 to 30 years participated in this study. Six females and 2 males were tested in experiment 1, and 4 females and 4 males were tested in experiment 2. All subjects had normal or corrected to normal vision. Informed consent was obtained from all subjects according to the Declaration of Helsinki and the guidelines of the local ethics committee of the medical faculty of the University of Tübingen, which approved the study.

Procedure and Stimulus Material

Subjects were seated upright in a magnetically shielded room (Vakuum-Schmelze, Hanau, Germany) and were instructed to sit as motionless as possible during the MEG recording. Stable posture was supported by a chinrest attached to the MEG chair. The computer-generated visual stimuli were rear projected onto a large translucent screen (digital light processing projector, frame rate 60 Hz, 800 × 600 pixels) positioned at a viewing distance of 92 cm in the magnetically shielded room. Viewing was binocular.

The visual stimulus consisted of 5 periods, each lasting 500 ms (see Fig. 1) and each being observed by the subjects during controlled stationary fixation. During the first 500 ms, only a stationary red dot (diameter 10 minarc) was presented in the middle of the screen which served as the fixation target and which remained visible for a total of 2 s. The first 500-ms period was followed by a second one introducing a random dot kinematogram (RDK) that covered a square of 16 × 16 degrees and was centered 15 degrees right (first experiment) or left (second experiment) of the fixation point. The RDK consisted of 1500 white squares (side length = 8 arcmin, lifetime = 1000 ms, dot density ~ 6 dots/degrees^2, luminance 47 cd/m^2) all moving incoherently, that is, in all possible directions with a resolution of 1 degree, at a common speed of 6 degrees/s. After the presentation of this first RDK that we will also refer to as the "prestimulus," a second RDK, the "test stimulus," started. The properties of this second RDK were identical to those described for the prestimulus except that a certain amount of dot elements moved coherently in the same direction (either to the left or to the right). Specifically, the percentage of coherently moving dots was 0%, 20%, 40%, 60%, 80%, or 100% of all dots in the individual trial. After a subsequent second fixation period, an arrow was presented in the middle of the screen pointing either to the left or to the right side as randomly chosen by the stimulus generator. Subjects were instructed to keep fixation as accurately as possible during the whole trial and to indicate by lifting their right or left index finger whether the motion direction of the dots of the test stimulus was identical (right index finger) or opposite (left index finger) to the pointing direction of the arrow. Subjects were instructed to guess if they were not sure about the direction seen (forced choice). Finger movements were detected using a light barrier. Note that the motor response could not be planned until the arrow had been presented, thus, guaranteeing that the MEG signals during the first 1000 ms after test stimulus onset were not related to movement preparation. The individual measurement consisted of 720 single trials with each coherence level (n = 6) being presented 120 times in a randomized sequence. In order to assess the ability to discriminate the motion direction embedded in noise, the percentage of correct responses in the individual measurement was plotted as function of motion coherence and fitted by a probit function. The perceptual threshold was defined by the coherence level for which the probit function predicted 75% correct responses. In a first experiment (see Fig. 1), 8 subjects were measured with the RDKs centered 15 degrees 'right' of the fixation point. In a second experiment, another group of 8 subjects was tested with the motion stimuli presented on the 'left' side.

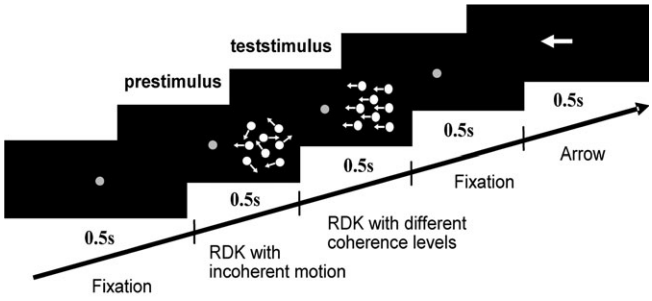

Figure 1. Time course of the stimulus. The stimulus consisted of 5 periods each lasting 500 ms. In contrast to the "prestimulus," a RDK consisting of incoherent motion, the following "test stimulus" involved the presentation of coherent motion the percentage of which was systematically varied between 0% and 100%. The coherent motion signal was directed either to the left or to the right. Subjects had to indicate whether the motion direction of the coherently moving dots of the test stimulus was identical or opposite to the pointing direction of the arrow presented at the end of the trial. For a first group of 8 subjects, the RDKs were presented right to the fixation dot. A second group of 8 subjects was stimulated with the RDKs located in the left visual field (not shown in the figure).

During all experiments, eye movements were monitored using a homemade video system taking the pupil's center as measure of eye position. Recordings were stored at a sampling rate of 50 Hz and analyzed off-line in order to assess the quality of fixation. In particular, the influence of visual motion coherence on the following oculomotor parameters was determined, that is, slow eye drifts (eye velocity), deviations from the fixation point (eye position), and the number and amplitude of saccades. To this end, the means of the different oculomotor measures were calculated for each of the 500-ms epochs of stimulation and in each subject. Then, these means were tested for dependencies on motion coherence by 1-way analyses of variance (ANOVAs) performed for each stimulus epoch, separately.

Recording and Analysis of the MEG Signals

Neuromagnetic activity was recorded using a whole-head MEG system (CTF Inc., Vancouver, Canada) comprising 151 first-order magnetic gradiometers. The signals were sampled at a rate of 625 Hz. Recording epochs lasted from stimulus onset to arrow offset plus 200 ms, leaving 2700 ms of recording time for each trial. The subject's head position was determined at the beginning and at the end of each recording session by means of localization coils fixed to the nasion and preauricular positions to ensure that head movements did not exceed channel separation.

Analysis of the Global Field Power

In a first attempt to search for MEG activity reflecting the amount of visual motion coherence, we analyzed the global field power (GFP). In order to obtain the GFP, the MEG recordings were first of all baseline corrected with respect to an interval ranging from 240 to 499 ms after stimulus onset which corresponded to the second half of the first interval of fixation preceding the presentation of the RDKs. The recordings were then digitally low-pass filtered at 40 Hz and averaged over the 120 trials for each coherence level and each subject using CTF software. Based on these averages, the GFP was calculated for each of the 6 coherence levels as the root of the mean-squared (RMS) magnetic fields of all 151 sensors for each sample and for each subject. Finally, in order to search for dependencies of the GFP on motion coherence, a (running) linear regression was calculated for each point in time testing for linear correlations between the RMS values and the coherence levels (MATLAB, version 6.5.1). Specifically, given the 6 coherence levels and the 8 subjects tested, each regression was based on 48 RMS values. In order to correct for multiple comparisons, at least 15 consecutive P values of the running regression were required to exceed a 0.01 level of significance (Rugg and others 1995).

Frequency Analysis of the MEG Recordings

In order to test whether correlations between MEG responses and visual motion coherence might be confined to specific frequency bands, a spectral analysis of the unfiltered MEG signals was performed. This analysis was conducted on single trial basis in the range of 1–100 Hz (1.23 Hz bins) for 5 partially overlapping 700-ms time windows. The time windows were defined by the 5 different 500-ms epochs of stimulation (compare Fig. 1) each being expanded by the 100-ms interval immediately preceding and following, respectively, the individual epoch. The resulting recording points were reduced to 218 and zero padded to obtain 256 points. To reduce the frequency leakage, the records were multiplied by Welch windows as recommended by Press and others (1992). A fast Fourier transform was calculated for each

time window, each channel, and each trial, separately. Then, spectral amplitudes (in the given time window) were averaged over all trials for each coherence level in each subject. The influence of motion coherence on the spectral amplitudes was assessed by an ANOVA (6 coherence levels) performed on the unaveraged group of the 8 subjects and for each frequency band (1.23 Hz) and channel (151), separately. Specifically, given the 6 coherence levels and the 8 subjects tested, each ANOVA was based on 48 spectral amplitude values. The *P* levels taken to be significant were adjusted by means of a Bonferroni correction given that the *P* values of 2 adjacent frequency bins had to be significant (Lutzenberger and others 2002). The critical level of statistical significance was, thus, calculated as

$$P = \sqrt{0.05/(\text{number of channels} \times \text{number of frequency bins})}$$
$$= \sqrt{0.05/(151 \times 100)}$$
$$= 0.0019.$$

Source Localization

As will be described in the Results section, we found that MEG signals in 2 different frequency domains depended on motion coherence. A first signal was observed in the low-frequency domain (1–3 Hz) and a second activation oscillated in the alpha band (~10 Hz). In order to localize these 2 components, different methods were used. The reason for choosing different methods for source localization was the following. Event-related cortical activity can either be time locked to stimulation and therefore will survive (or will be enhanced by) averaging or, alternatively, be only loosely time locked and, hence, will be detectable only by analyses based on single trials (Klimesch and others 1998). Evoked cortical activity that is time locked can usually be localized appropriately by applying conventional dipole models. Activity that is not phase locked to stimulation, however, requires alternative approaches of source localization such as offered by synthetic aperture magnetometry (SAM) (Robinson and Vrba 1999). In order to test whether the 2 MEG signals correlating with motion coherence in this study were either phase locked or not and, thereby, which procedure for source localization would be appropriate, the ANOVA described above was also applied to the averaged MEG signals.

The effect of motion coherence on the activity in the low-frequency domain (1–3 Hz) survived averaging, thus, indicating that this component was phase locked. Accordingly, a conventional dipole model approach was chosen for source localization. Single equivalent current dipoles (ECDs) were estimated for the group averages as well as for the single subjects based on the differences between the MEG responses obtained for the highest (100%) and the lowest coherence level (0%). First, the differences between 100% and 0% were calculated for each subject separately by subtracting the MEG response elicited by the 0% coherence level (raw data were baseline corrected, 40 Hz low-pass filtered, and averaged over trials for each subject separately) from the response obtained from the 100% coherence condition. For the group analysis, these differences were then averaged over the subjects. In other words, in a first step, only the differential activity was modeled. ECDs were determined by conventional least-square minimization procedures and based on an individual spherical head model, derived from anatomic magnetic resonance images of one of the subjects. In a second step and in order to exclude the possibility that the dipole solution derived from the difference between conditions might not be a true reflection of the primary activation or might be specific for the comparison of 2 extremes, dipole source analysis was also performed for the 100% coherence condition and one further difference (20% vs. 100% coherence).

In contrast to the MEG activity in the low-frequency band, the alpha oscillation showed a significant dependency on motion coherence only when the signals were not averaged prior to analysis. For this reason, the alpha activation was not considered phase locked and therefore localized by means of a beamformer algorithm. To this end, 3-dimensional imaging of brain activity was performed using SAM (Robinson and Vrba 1999). SAM is a type of minimum variance beamformer that is sensitive for 4 dimensions (voxel location and source orientation) and therefore might result in a better spatial resolution as compared with conventional beamformers (for details see, e.g., Vrba and Robinson 2002). This specific type of minimum variance beamformer, implemented in the CTF software, was calculated for the 9- to 12-Hz frequency band in the fixation period after motion presentation (1.5–2.0 s). For each subject, a pseudo *t* statistic was calculated to estimate the difference in source power between the 0% and 100% coherence condition at the given target voxel (voxel side length 1 cm; Robinson and Vrba 1999).

Results

The results of the 2 experiments testing MEG responses as function of visual motion coherence were qualitatively the same. This was expected because the 2 experiments differed only in the visual hemifield stimulated (experiment 1: right hemifield; experiment 2: left hemifield) and were repeated most of all to test the reliability of the results. The similarity of results of the 2 experiments applied to both the psychophysical/behavioral and the electrophysiological results. More precisely, the motion discrimination thresholds did not differ between the 2 groups tested as indicated by a group mean being 17.5% in the first and 27.5% in the second group ($P = 0.19$). The somewhat higher mean in the second experiment, albeit nonsignificant, was due to one outlier. Exclusion of this outlier in experiment 2 resulted in a mean of 17.5%, that is, in the same mean as obtained from experiment 1. Moreover, an influence of visual motion coherence on the quality of fixation could be detected in neither of the 2 experiments. Specifically, ANOVAs did not show any significant effect of motion coherence on the different oculomotor parameters considered such as slow eye drifts (eye velocity), deviations from the fixation point (eye position), or the number and amplitude of saccades ($P > 0.05$, each). In other words, by excluding the possibility that significant eye movements had been elicited by the presentation of the coherent motion stimuli, it was assured that differences in the MEG responses would not reflect oculomotor artifacts. In the following, these electrophysiological differences will first be presented in more detail for experiment 1.

Influence of Visual Motion Coherence on the GFP

As stated in the Materials and Methods section, in a first step, the GFP was analyzed in order to search for MEG activity correlating with visual motion coherence. As shown in Figure 2A, the power of the global MEG response as assessed by the RMS values started to diverge into higher and lower values for different coherence levels shortly after test stimulus onset. For instance, 210 ms after coherent motion onset, that is, at the peak latency of the MEG response, the GFP elicited by the 100% coherent motion stimulus was 55% higher than the GFP observed for the 0% coherent stimulus. The positive correlation between GFP and motion coherence that can also be derived from the positive slope (=beta value) of the running linear regression (see middle panel of Fig. 2A) started to be significant 172 ms after test stimulus onset (lower panel of Fig. 2A). Although this correlation was most robust for the group average, it was present also in the individual subjects as shown in Figure 2B plotting the GFPs of both the group and the single subjects averaged for a 100-ms time interval starting 200 ms after test stimulus onset. The same result was obtained from experiment 2 stimulating the left visual field with the one difference that the correlation between GFP and motion coherence emerged somewhat later (254 ms after test stimulus onset).

Frequency Analysis and Source Localization

Spectral analysis revealed MEG signals in 2 different frequency domains depending on motion coherence. A first signal was

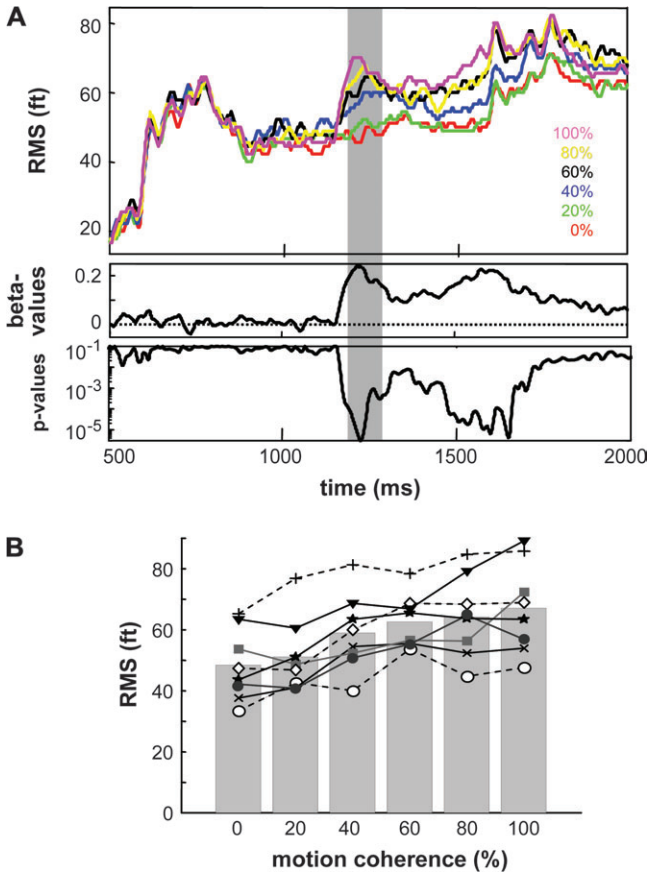

Figure 2. Dependency of the GFP on visual motion coherence. (A) RMS values averaged over the 8 subjects are plotted for the 6 coherence levels (indicated by different colors) as function of time. The *x* axis starts with the presentation of the first RDK (incoherent motion, onset at 500 ms) followed by the test stimulus comprising coherent motion of varied strength (onset at 1000 ms). The lower panels show the beta and *P* values, respectively, obtained from a linear regression between RMS values and motion coherence for each sample point. (B) GFP as function of motion coherence averaged for a 100-ms interval starting 200 ms after test stimulus onset (indicated by the gray area in A). Results of the group (bars) and of the individual subjects (symbols, lines) both reveal a consistent positive correlation between RMS values and motion coherence.

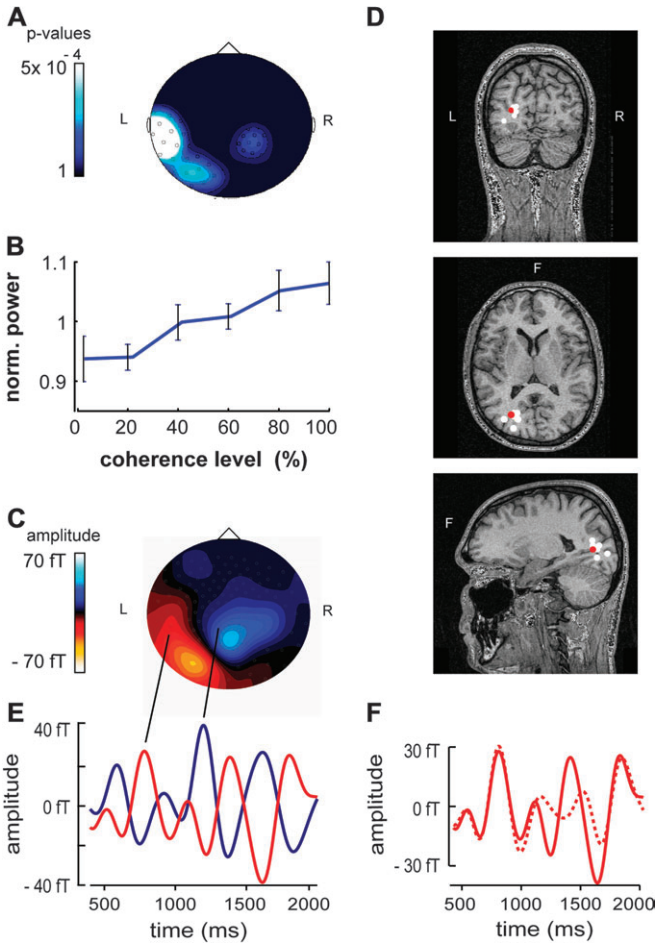

Figure 3. Spectral power in the 3-Hz frequency band during coherent motion presentation correlates with motion coherence. (A) Statistical probability mapping of spectral amplitude dependencies on motion coherence projected onto a 2-dimensional MEG sensor map (seen from above, nose up). *P* values denoting the level of statistical significance of the effect of motion coherence on the spectral amplitude were calculated from an ANOVA and are color-coded here in order to provide a quasi-field distribution. R, right; L, left; F, frontal. (B) Spectral power in the 3-Hz frequency band averaged over all channels with *P* values ≤ 0.0019 as function of motion coherence. The *y* axis denotes the means and standard deviations of the spectral power for the group of 8 subjects. Before assessing the group statistics, spectral amplitudes for the different coherence levels were normalized in the individual subject based on the mean spectral amplitude obtained from all coherence levels. (C) Magnetic field map of the group difference between MEG signals obtained for the 0% and 100% coherent motion conditions (166 ms after test stimulus onset). (D) Dipole solutions of the differential activity depicted in (C). The red dot marks the dipole obtained from the group analysis, and the white dots delineate the location of dipole solutions derived from 6 out of 8 subjects. (E) 3 ± 2 Hz Gaussian filtered time course of MEG activity recorded from 2 sensors (marked in C with 2 lines and held distinguishable by 2 different colors) for the 100% coherence condition. The coherent stimulus started at 1000 ms. (F) 3 ± 2 Hz Gaussian filtered time course of activity recorded from the left sensor as depicted in red in Figure 3E. The solid line shows the oscillatory activity for this sensor elicited by the 100% coherence condition as compared with the 0% coherence condition (dashed line).

observed for the time window of test stimulus presentation and a second one in the fixation period following the presentation of coherent motion.

The first MEG component was obtained in the 3-Hz frequency band and was picked up from temporo-occipital sensors located contralateral to the stimulated visual hemifield (Fig. 3A). As shown in Figure 3B, the dependency of the spectral power in this frequency range was positive for these channels, that is, spectral power increased monotonically with increasing motion coherence similar to the changes in GFP observed in this time window. Indeed, the distribution of the sensors with significant effects (Fig. 3A) resembled very much the magnetic field distribution of the group difference between the MEG responses obtained for the highest (100%) and the lowest coherence level (0%) depicted in Figure 3C, thus, suggesting that the differences in the GFP reflected this low-frequency component. As justified in the Materials and Methods section, this MEG signal was modeled by assuming a single ECD whose 3-dimensional location and orientation were estimated by applying the analysis to the difference between MEG signals obtained for the 0% and 100% coherent motion conditions. Dipole solutions were calculated for the grand average of all subjects and, additionally, separately for each subject. Dipoles were considered to be adequate if they explained a minimum of 70% signal variance. As shown in Figure 3D, the differential neuromagnetic activity observed for the group could be adequately described by assuming a single ECD (174 ms after coherent motion onset) in left temporo-occipital cortex (Talairach

coordinates: $x = -27.5$, $y = -68.7$, $z = 11.0$) close to area MT (V5) + as delineated in numerous imaging studies (e.g., Watson and others 1993; Previc and others 2000). Dipole solutions derived from single subjects confirmed this conclusion with coordinates close to those obtained from the group data ([means ± standard deviations]: $x = -24.8 \pm 4.4$, $y = -74.2 \pm 7.9$, $z = 12.4 \pm 5.8$). Dipoles were located contralateral to the visually stimulated hemifield in all subjects. For 2 subjects, no single dipole solution was feasible because the differential activity in these 2 subjects was too small. While the variance of the differential magnetic field explained by the dipole model was higher than 70% for the first 230 ms after test stimulus onset, the following activity was not sufficiently explained by a single ECD located in temporo-occipital cortex. The following activity, however, was too variable in the individual subjects to allow for reliable source localization. The dipole fitted to the group difference between the 100% and 20% motion coherence condition ($x = -39$, $y = -64$, $z = 19.8$; 174 ms after coherent motion onset; explained variance > 86%) and to the group data obtained from the 100% coherence condition ($x = -34$, $y = -75$, $z = 13$; explained variance > 80%) exhibited very similar coordinates as those derived from the first comparison (difference between 100% and 0% coherence).

The second MEG signal depending on motion coherence was observed in the 10-Hz frequency band and was present only in the fixation period following the offset of coherent motion presentation. This neuromagnetic activity being statistically significantly modulated by motion coherence was picked up from channels covering the occipital region (Fig. 4A). As can be derived from Figure 4B, the spectral power in the 10-Hz band decreased monotonically with increasing coherence. As explained in the Materials and Methods section, instead of a dipole model, a beamforming method was used in order to localize this activity. To this end, first the source power was calculated for the 9- to 12-Hz frequency band during the fixation period after the test stimulus using SAM (for details, see Materials and Methods). Second, the difference in source power between the 0% and 100% coherence level was calculated applying pseudo t statistics. Figure 4C shows that voxels with the maximum t values ($t \geq 4.8$) were located in occipital cortex indicating an activation of early visual cortex such as areas V1 and V2 ($x = 1.7 \pm 22.2$, $y = -88.2 \pm 6.12$, $z = 15.2 \pm 10.1$). For 2 out of 8 subjects, SAM revealed no voxels with significantly higher activations for the incoherent motion condition. No effects could be found in the theta or beta frequency range.

Experiment 2 in which the visual motion stimuli were presented in the left hemifield replicated the results of the first experiment. Briefly, the 2 main observations, that is, demonstration of neuromagnetic activity in the 3-Hz frequency band positively correlating with motion coherence and of a second activity in the alpha band negatively correlating with motion coherence were replicated (Fig. 5). Identical to experiment 1, the low-frequency activity was present during motion presentation, whereas the alpha modulation was observed after motion offset. Dipole solutions again suggested contralateral area MT (V5) + as the main neuronal substrate of the low-frequency activity ($x = 26.7 \pm 7.5$, $y = 71.3 \pm 15.9$, $z = 10.9 \pm 10.1$). Dipoles were located contralateral to the visually stimulated hemifield in all subjects. In turn, the alpha activation could be attributed to early visual cortex ($t \geq 1.9$; $x = 9.4 \pm 8.9$, $y = -92.7 \pm 11.1$, $z = 9.6 \pm 15.3$) with the one difference to experiment 1 being that it seemed to be more clearly confined to the hemisphere contralateral to stimulation. For 3 out of 8 subjects, SAM revealed no voxels with significantly higher activations for the incoherent motion condition. Finally, in neither experiment 1 nor experiment 2, any neuromagnetic activity in the gamma range was observed correlating with motion coherence as might have been expected considering

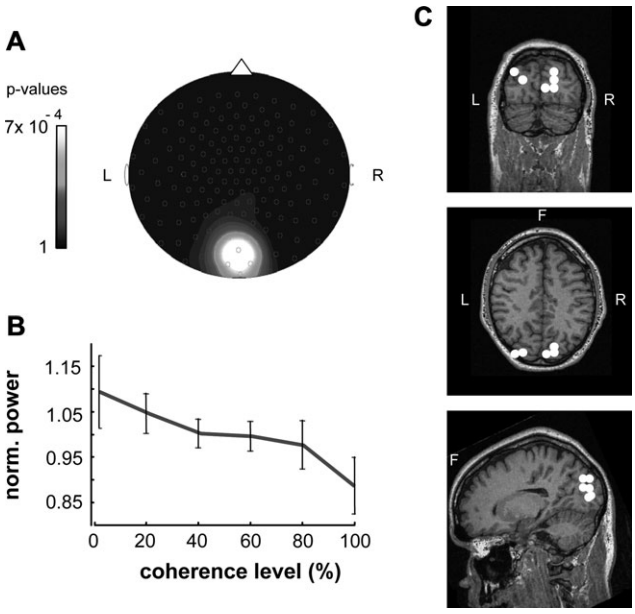

Figure 4. Spectral power in the 10H-z frequency band after coherent motion offset correlates with motion coherence. (A) Statistical probability mapping of spectral amplitude dependencies on motion coherence projected onto a 2-dimensional MEG sensor map (same conventions as in Fig. 3A). (B) Means and standard deviations of the spectral power in the 10-Hz band for the group of 8 subjects as function of motion coherence (same conventions as in Fig. 3B). (C) Localization of voxels with maximum t values obtained from pseudo t statistics estimating the difference in source power between the 0% and 100% coherence condition (results from 6 out of 8 subjects). Source power was obtained using a minimum variance beamformer (SAM) for the 9- to 12-Hz frequency band.

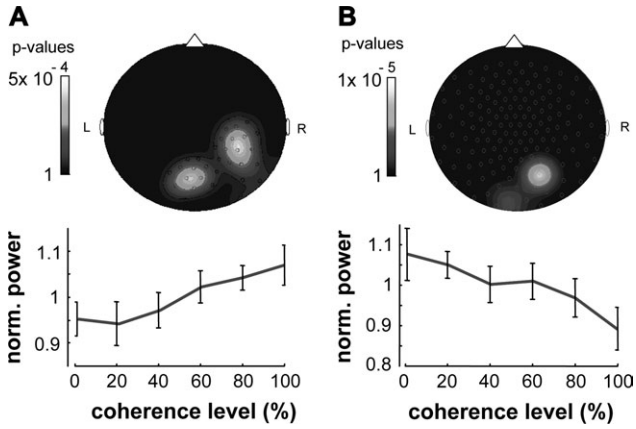

Figure 5. Correlations of spectral power with motion coherence for experiment 2 (visual motion presented in the left hemifield). (A) Spectral power in the 3-Hz frequency band during coherent motion presentation positively correlates with motion coherence. (B) Spectral power in the 10-Hz frequency band after coherent motion offset negatively correlates with motion coherence. Upper panels: Statistical probability mapping of spectral amplitude dependencies on motion coherence projected onto a 2-dimensional MEG sensor map (same conventions as in Figs 3A and 4A). (B) Means and standard deviations of the spectral amplitudes for the group of 8 subjects as function of motion coherence (same conventions as in Figs 3B and 4B).

the work of Siegel and others (2006) who applied a much larger number of trials.

Discussion

Whereas single-cell recordings in nonhuman primates have yielded intriguing insights into the mechanisms underlying visual motion perception by testing how neuronal responses of selected cortical areas vary with the characteristics of visual motion, human studies measuring brain activity as function of motion strength are rare. This study was performed in order to provide a full description of the dependencies of spectral powers of brain activity on motion coherence in man. To this end, a modified delayed match-to-sample paradigm was chosen that allowed to disentangle visual stimulation from motor response preparation. Moreover, by excluding eye movement dependencies on motion coherence, changes in the neuromagnetic responses could be attributed without doubt to changes directly related to the cortical processing of the physical attributes of the stimulus. Finally, the results could be replicated in 2 independent series of experiments, thus, extensively excluding the possibility of statistical errors due to multiple comparisons inherent to human brain imaging studies.

A first finding of this study was that neuromagnetic responses attributed to human area MT+ linearly increased with motion coherence. At first glance, this result may not be surprising because MT neurons have been shown to linearly increase firing rate with motion coherence in various single-cell recording studies (e.g., Zeki 1974; Maunsell and Van Essen 1983; Newsome and others 1989; Britten and others 1992; Britten and Newsome 1998). Yet, human studies performed so far have not consistently demonstrated that activity of human area MT+ reflects the strength of visual motion. On the one hand, Rees and others (2000) using fMRI and Aspell and others (2005) using MEG could show a positive correlation between motion coherence and activation in area MT+. Likewise, Braddick and others (2001; fMRI) observed a stronger MT+ activation for coherent as compared with incoherent motion. On the other hand, however, some studies found no or even a reverse relationship between motion coherence and activity in MT+ (fMRI, McKeefry and others 1997; MEG, Lam and others 2000).

The differences between the results of these studies might at least partly be explained by stimulus parameters (e.g., dot density) as discussed in detail by Braddick and others (2001). Low dot densities such as used by McKeefry and others (1997) or Lam and others (2000) who demonstrated higher activations for noise stimuli might not be sufficient for summation of the response under the coherent motion condition. In line with this interpretation, the dot density used here was roughly 30 times higher than the one used for instance by McKeefry and others (1997). As discussed by Aspell and others (2005), also stimulus size may play an important role. The reason is that visual stimuli used in human studies are not confined to the classical receptive field of neurons in area MT, that is, for the majority of neurons, at least parts of their surrounds are stimulated with the consequences of center-surround interactions that on average may tend to be inhibitory (Allman and others 1985; Born and Tootell 1992). We cannot validate this hypothesis because our stimulus (16°) exceeded the mean receptive field size (9°) of monkey MT for the eccentricity chosen (Albright and Desimone 1987). In summary, dot density rather than stimulus size seems likely to have important influences on the differential population responses to visual motion, but their specific impact remains to be specified by further studies.

Most of the human studies addressed so far found more areas than area MT+ alone to be influenced by motion coherence including area V3a, the intraparietal and superior temporal sulcus (Braddick and others 2001; Aspell and others 2005), or V1/V2 (McKeefry and others 1997). Rees and others (2000) supplying the most detailed description of dependencies of blood oxygen level–dependent responses on motion coherence so far reported bilateral activity in areas MT+, kinetic occipital, and V2 as well as activation in the right fusiform gyrus, left occipital gyrus, and left middle occipital gyrus to increase for higher motion coherence. Conversely, activity in right anterior cingulate and left insula was found to negatively depend on motion coherence. As stated in the Results section, also in this study, the brain activity reflecting motion coherence was not restricted to area MT+ because correlating responses were observed more than 230 ms after test stimulus onset, that is, definitely after the interval for which the differential activity could be sufficiently modeled by a single (MT+) dipole. This correlating activity following the MT+ response, however, could not be adequately localized due to large individual differences and low signal-to-noise ratios.

An increase in activity by motion coherence could not only be shown for the RMS values (i.e., activity averaged over trials) but also for the raw data in a 3-Hz frequency band. In order to test whether this latter effect was a reflection of a sustained slow frequency oscillation or, alternatively, a classically evoked potential, we looked at the time course of the 3 ± 2–Hz Gaussian filtered MEG signals as exemplified for 2 channels (LT25, RP11) in Figure 3E. As can be seen from this figure, the 3-Hz oscillations already started during the presentation of the incoherent motion (onset 500 ms) persisted at least until the end of the second fixation period (2000 ms) and therefore did not reflect motion stimulus on- or offset. Its modulation (see Fig. 3F), however, was triggered by the presentation of the coherent motion stimulus (onset at 1000 ms). On the basis of our results, we can answer neither the question whether these oscillations may also be present in the absence of visual stimulation nor the question whether it might critically depend on the temporal sequence of the stimulus used. As far as we can tell, an oscillation in the delta band (3 Hz) correlating with properties of external stimuli has not been reported so far, and its specific role remains to be further investigated.

Spectral analyses disclosed a second component which has not been reported so far in either human or monkey studies. This second component, arising from early visual cortex and oscillating in the alpha band, followed motion stimulus offset and showed a negative correlation with motion coherence.

Alpha oscillations have struck scientists since the discovery of the electroencephalography (EEG) by Hans Berger in the late twenties of the last century (Berger 1929), and its properties and subclasses have been described extensively in many EEG and MEG studies (for review, see Pfurtscheller and others 1996, 1999; Klimesch 1999). Since the work of Berger, it has been suggested that visual (or other sensory) task demands and visual attention in particular (e.g., Maruffo and others 2001) are the primary factors that lead to a suppression of the alpha rhythm. This traditional view is obviously at odds with our finding of alpha synchronization emerging for the lower motion coherence levels. The reason is that the attentional load in our experiment—if at all—was highest in trials with low motion

coherence because those were the most demanding. Moreover, one might expect a dependency of alpha power during motion presentation rather than after motion offset.

In order to resolve this seeming paradox, we have to consider more recent work that indeed has prepared the ground for a paradigm shift in the current conception of alpha oscillations. In contrast to the earlier notion that alpha synchronization indexes "cortical idling," that is, a default resting state, it is becoming apparent that alpha oscillations indicate an active mechanism suppressing cortical activity that might interfere with task-relevant signal processing (e.g., Ward 2003). In line with this interpretation, recent studies have shown that alpha desynchronization is a local phenomenon that occurs specifically over task-relevant cortical areas, whereas task-irrelevant regions show a pronounced synchronization (Klimesch and others 1999). This conclusion has been derived among others from studies directly testing alpha activity for different conditions of directed attention. For instance, Foxe and others (1998) using an intermodal selective attention paradigm found that a visual cue indicating an upcoming auditory stimulus increased alpha activity over parieto-occipital cortex arguably reflecting disengagement of the visual attentional system. The opposite result, that is, a decrease in occipital alpha power, was obtained when the cue announced a visual target. A later study of the same group (Fu and others 2001) reported that this kind of occipital alpha modulation can also be induced by cross-modal (auditory) cues. Eventually, Worden and others (2000) could demonstrate that spatial shifts of visual attention were paralleled by sustained focal increases of alpha synchronization in a retinotopically specific manner: increases in alpha activity were seen only over occipital cortex contralateral to the direction of the to-be-ignored location. Taken together, these experiments suggest that alpha synchronization reflects active gating of uncued sensory modalities or spatial locations, respectively. The notion that alpha oscillations might indicate early inhibition of disturbing sensory input information as a part of the process of focusing attention on relevant information has been widened on the basis of studies not directly devoted to attention. For instance, Klimesch and others (1999) using a memory search paradigm described an increase in the alpha band with higher task difficulty over occipital cortex after the presentation of a set of letters that had to be memorized. Likewise, Jensen and others (2002) reported a positive correlation between alpha band amplitude and memory load using a modified Sternberg task. Interestingly, these effects were restricted to the memory retention phase pointing to the possibility that alpha activation might play an important functional role by preventing any flow of disturbing information into areas retaining memory items. Based on their observations, Klimesch and others (1999) suggested that alpha synchronization might in general reflect a mechanism that increases signal-to-noise ratios within the cortex by means of inhibition of unnecessary or conflicting processes to the task at hand. In other words, alpha synchronization could indicate a more generalized inhibition of task-irrelevant cortical areas.

In a similar way, occipital alpha activity increasing with lower motion coherence after motion offset seems ideally suited to protect the integration of visual motion signals in later areas from upcoming disturbing input. There is ample evidence that during the formation of a perceptual decision in a motion direction discrimination task, sensory evidence is integrated over time and accumulates until a critical threshold is reached—the weaker the sensory evidence the longer the integration will last (e.g., Snowden and Braddick 1991; Britten and others 1992; Patzwahl and Zanker 2000). Thus, with decreasing motion coherence, the processing of motion direction information becomes not only more time consuming but also more sensitive to noise and therefore may benefit the more from gating mechanisms in early visual cortex impeding new signals from interfering with ongoing signal processing in higher order areas such as area MT+. In line with the findings of Klimesch and others (1999) or Jensen and others (2002), this integration may include memorization of the stimulus seen.

As outlined earlier, the seeming paradox that alpha activity (assumed to reflect inactivation) may increase with task demand can be resolved only if one assumes that this activity is spatially restricted. Indeed, the field distribution and source localization (see Figs 4 and 5) revealed that the modulation of alpha oscillations was confined to early visual cortex, whereas the GFP after test stimulus offset was still higher for coherent motion stimuli as compared with motion noise (Fig. 2A). This finding is in favor of the more specific interpretation that alpha oscillations might reflect an active gating mechanism implemented most of all—if not exclusively—in early sensory areas of the brain. Because neuromagnetic activity of primary visual cortex in our study did not depend on motion coherence during motion presentation, we have to assume that the information on signal strength and, thus, on the need to enforce occipital gating, is not extracted by primary visual cortex itself but more likely is back propagated from later specialized cortical areas such as area MT+ (Hupe and others 1998).

Conclusions

In conclusion, we could reveal 2 electrophysiological correlates of visual motion coherence in man using MEG. A first MEG signal positively correlated with motion coherence during stimulus presentation could be attributed to extrastriate cortex including area MT+. The dependency of activity in human area MT+ on motion coherence reinforces the importance of this area in generating a percept of global motion and supports the notion that human and nonhuman primates share a similar visual motion system. A second MEG signal depending on motion coherence was an occipital oscillation in the alpha band whose amplitude decreased with motion strength after motion offset. We interpret this second signal as a reflection of an active gating mechanism that protects the ongoing processing of visual motion information in extrastriate cortical areas.

Notes

This work was supported by Deutsche Forschungsgemeinschaft (SFB 550, TP A2, A7, C1), Graduiertenkolleg Kognitive Neurobiologie, and Schilling Foundation. *Conflict of interest*: None declared.

Address correspondence to Thomas Haarmeier, MD, Department of General Neurology, Hertie-Institute for Clinical Brain Research, Klinikum Schnarrenberg, Hoppe-Seyler-Straße 3, 72076 Tübingen, Germany. Email: thomas.haarmeier@uni-tuebingen.de.

References

Albright T, Desimone R. 1987. Local precision of visuotopic organization in the middle temporal area (MT) of the macaque. Exp Brain Res 65:582–592.

Allman J, Miezin F, McGuinness E. 1985. Stimulus specific responses from beyond the classical receptive field: neurophysiological mechanisms for local-global comparisons in visual neurons. Ann Rev Neurosci 8:407–430.

Aspell JE, Tanskanen T, Hurlbert AC. 2005. Neuromagnetic correlates of visual motion coherence. Eur J Neurosci 22:2937–2945.
Berger H. 1929. Über das Elektroenkephalogramm des Menschen. Arch Psychiatr Nervenkr 87:527–570.
Born T, Tootell R. 1992. Segregation of global and local motion processing in primate middle temporal visual area. Nature 357:497–499.
Braddick OJ, O'Brien JMD, Wattam-Bell J, Atkinson J, Hartley T, Turner R. 2001. Brain areas sensitive to coherent visual motion. Perception 30:61–72.
Britten KH, Shadlen MN, Newsome WT, Movshon JA. 1992. The analysis of visual motion: a comparison of neuronal and psychophysical performance. J Neurosci 12:4745–4765.
Britten KH, Newsome WT, Shadlen MN, Celebrini S, Movshon JA. 1996. A relationship between behavioral choice and the visual responses of neurons in macaque MT. Vis Neurosci 13:87–100.
Britten KH, Newsome WT. 1998. Tuning bandwidth for near-threshold stimuli in area MT. J Neurophysiol 80:762–770.
Foxe JJ, Simpson GV, Ahlfors SP. 1998. Parieto-occipital ~10 Hz activity reflects anticipatory state of visual attention mechanisms. Neuroreport 9:3929–3933.
Fu KG, Foxe JJ, Murray MM, Higgins BA, Javitt DC, Schroeder CE. 2001. Attention-dependent suppression of distracter visual input can be cross-modally cued as indexed by anticipatory parieto-occipital alpha-band oscillations. Cogn Brain Res 12:145–152.
Gold JI, Shadlen MN. 2000. Representation of a perceptual decision in developing oculomotor commands. Nature 404:390–394.
Gold JI, Shadlen MN. 2003. The influence of behavioral context on the representation of a perceptual decision in developing oculomotor commands. J Neurosci 23(2):632–651.
Horwitz GD, Newsome WT. 1999. Separate signals for target selection and movement specification in the superior colliculus. Science 284:1158–1161.
Hupe J, James A, Payne B, Lomber S, Girard P, Bullier J. 1998. Cortical feedback improves discrimination between figure and background by V1, V2 and V3 neurons. Nature 394:734–787.
Jensen O, Gelfand J, Kounios J, Lisman JE. 2002. Oscillations in the alpha band (9–12 Hz) increase with memory load during retention in a short-term memory task. Cereb Cortex 12:877–882.
Kim JN, Shadlen MN. 1999. Neural correlates of a decision in the dorsolateral prefrontal cortex of macaque. Nat Neurosci 2:176–184.
Klimesch W, Russegger H, Doppelmayr M, Pachinger T. 1998. A method for the calculation of induced band power: implications for the significance of brain oscillations. Electroencephalogr Clin Neurophysiol 108(2):123–130.
Klimesch W. 1999. EEG alpha and theta oscillations reflect cognitive and memory performance: a review and analysis. Brain Res Rev 29 (2–3):169–195.
Klimesch W, Doppelmayr M, Schwaiger J, Auinger P, Winkler T. 1999. 'Paradoxical' alpha synchronization in a memory task. Cogn Brain Res 7(4):493–501.
Lam K, Kaneoke Y, Gunji A, Yamasaki H, Matsumoto E, Naitos T, Kakigi R. 2000. Magnetic response of human extrastriate cortex in the detection of coherent and incoherent motion. Neuroscience 97:1–10.
Lutzenberger W, Ripper B, Busse L, Birbaumer N, Kaiser J. 2002. Dynamics of gamma-band activity during an audiospatial working memory task in humans. J Neurosci 22:5630–5638.
Maruyama K, Kaneoke Y, Watanabe K, Kakigi R. 2002. Human cortical responses to coherent and incoherent motion as measured by magnetoencephalography. Neurosci Res 44:195–205.
Marrufo MV, Vaquero E, Cardoso MJ, Gomez CM. 2001. Temporal evolution of α and β bands during visual spatial attention. Cogn Brain Res 12:315–320.
Maunsell JHR, Van Essen DC. 1983. Functional properties of neurons in middle temporal visual area of the macaque monkey. I. Selectivity for stimulus direction, speed, and orientation. J Neurophysiol 49:1127–1147.
McKeefry DJ, Watson JDG, Frackowiak RSJ, Fong K, Zeki S. 1997. The activity in human area V1/V2, V3 and V5 during the perception of coherent and incoherent motion. Neuroimage 5:1–12.
Nakamura H, Kashii S, Nagamine T, Matsui Y, Hashimoto T, Honda Y, Shibasaki H. 2003. Human V5 demonstrated by magnetoencephalography using random dot kinematograms of different coherence levels. Neurosci Res 46(4):423–433.
Newsome TW, Kenneth H, Britten KH, Movshon JA. 1989. Neuronal correlates of a perceptual decision. Nature 341:52–54.
Patzwahl DR, Zanker JM. 2000. Mechanisms of human motion perception: combining evidence from evoked potentials, behavioural performance and computational modelling. Eur J Neurosci 12: 273–282.
Pfurtscheller G, Stancak A Jr, Neuper C. 1996. Event-related synchronization (ERS) in the alpha band—an electrophysiological correlate of cortical idling: a review. Int J Psychophysiol 24(1–2):39–46.
Pfurtscheller G, Lopes da Silva FH. 1999. Event-related EEG/MEG synchronisation and desynchronisation: basic principles. Clin Neurophysiol 110:1842–1857.
Press WH, Teukolsky SA, Vetterling WT, Flannery BP. 1992. Numerical recipes. Cambridge, UK: Cambridge University Press. p 547.
Previc FH, Liotti M, Blakemore C, Beer J, Fox P. 2000. Functional imaging of brain areas involved in the processing of coherent wide field-of-view visual motion. Exp Brain Res 131:393–405.
Rees G, Friston K, Koch C. 2000. A direct quantitative realtionship between the functional properties of human and macaque V5. Nat Neurosci 3:716–723.
Robinson SE, Vrba J. 1999. Functional neuroimaging by synthetic aperture magnetometry (SAM). In: Yoshimoto T, Kotani M, Kuriki S, Kuribe H, Nakasato N, editors. Recent advances in biomagnetism. Sendai: Tohoku University Press. p 302–305.
Roitman JD, Shadlen MN. 2002. Response of neurons in the lateral intraparietal area during a combined visual discrimination reaction time task. J Neurosci 22(21):9475–9489.
Rugg MD, Doyle MC, Well T. 1995. Word and non-word repetition within- and across-modality: an event-related potential study. J Cogn Neurosci 7:209–227.
Shadlen MN, Britten KH, Newsome WT, Movshon JA. 1996. A computational analysis of the realtionship between neuronal and behavioural responses to visual motion. J Neurosci 15:3870–3896.
Shadlen MN, Newsome WT. 2001. Neural basis of a perceptual decision in the parietal cortex (area LIP) of the rhesus monkey. J Neurophysiol 86:1916–1936.
Siegel M, Donner T, Oostenveld R, Fries P, Engel A. 2006. High-frequency activity in human visual cortex is modulated by visual motion strength. Cereb Cortex 10.1093/cercor/bhk025.
Snowden RJ, Braddick OJ. 1991. The temporal integration and resolution of velocity signals. Vision Res 31(5):907–914.
Vrba J, Robinson SE. 2002. Differences between synthetic aperture magnetometry and linear beamformers. In: Nenonen J, Ilmoniemi RJ, Katila T, editors. Biomag 2000, Proceedings of the 12th International Conference on Biomagnetism. Espoo, Finland: Helsinki University of Technology, 2001, p. 681–684.
Ward LM. 2003. Synchronous neural oscillations and cognitive processes. Trends Cogn Nuerosci 7(12):553–559.
Watson JD, Myers R, Frackowiak RS, Hajnal JV, Woods RP, Mazziotta JC, Shipp S, Zeki S. 1993. Area V5 of the human brain: evidence from a combined study using positron emission tomography and magnetic resonance imaging. Cereb Cortex 3(2):79–94.
Worden MS, Foxe JJ, Wang N, Simpson GV. 2000. Anticipatory biasing of visuospatial attention indexed by retinotopically specific alpha-band; electroencephalography increases over occipital cortex. J Neurosci 20:RC63 1–6.
Zeki SM. 1974. Functional organisation of a visual area in the posterior bank of the superior temporal sulcus of the rhesus monkey. J Physiol 236:549–573.